Force detection of high-frequency electron paramagnetic resonance spectroscopy of microliter solution sample

Okamoto, Tsubasa ; Takahashi, Hideyuki ; Ohmichi, Eiji ; Ishikawa, Haruto ; Mizutani, Yasuhisa ; Ohta, Hitoshi

(Citation)
Applied Physics Letters,113(22):223702-223702

(Issue Date)
2018-11

(Resource Type)
journal article

(Version)
Version of Record

Applied Physics Letters

Force detection of high-frequency electron paramagnetic resonance spectroscopy of microliter solution sample

Cite as: Appl. Phys. Lett. **113**, 223702 (2018); https://doi.org/10.1063/1.5055743
Submitted: 10 September 2018 . Accepted: 08 November 2018 . Published Online: 28 November 2018

Tsubasa Okamoto, Hideyuki Takahashi, Eiji Ohmichi, Haruto Ishikawa, Yasuhisa Mizutani, and Hitoshi Ohta

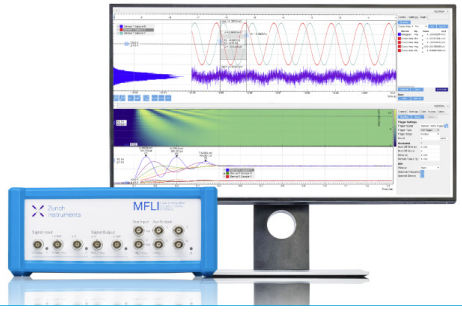

Force detection of high-frequency electron paramagnetic resonance spectroscopy of microliter solution sample

Tsubasa Okamoto,[1] Hideyuki Takahashi,[2] Eiji Ohmichi,[1,a)] Haruto Ishikawa,[3] Yasuhisa Mizutani,[3] and Hitoshi Ohta[4]
[1]*Graduate School of Science, Kobe University, 1-1 Rokkodai, Nada, Kobe 657-8501, Japan*
[2]*Organization for Advanced and Integrated Research, Kobe University, 1-1 Rokkodai, Nada, Kobe 657-8501, Japan*
[3]*Graduate School of Science, Osaka University, 1-1 Machikaneyama, Toyonaka 560-0043, Japan*
[4]*Molecular Photoscience Research Center, Kobe University, 1-1 Rokkodai, Nada, Kobe 657-8501, Japan*

(Received 10 September 2018; accepted 8 November 2018; published online 28 November 2018)

Force detection of magnetic resonance is now able to attain extremely high spin sensitivity. In these setups, microcantilevers were usually used as a sensitive force sensor and, in most cases, have been applied to solid-state samples such as paramagnetic impurities in solids. On the other hand, there are now growing demands for their applications to liquid-state samples in the research areas of life science because many proteins and enzymes are biofunctionally active only in solutions, where they interact with the surrounding water molecules. In this letter, we present an electron paramagnetic resonance (EPR) technique for solution samples using a SiN_x nanomembrane and report high-frequency EPR spectroscopy of a microliter-volume frozen solution sample of hemin and myoglobin at multiple frequencies up to 350 GHz. This technique would be particularly useful to obtain more detailed insight into the electronic structure of metalloproteins/metalloenzymes under biologically active conditions. *Published by AIP Publishing.*
https://doi.org/10.1063/1.5055743

Force detection of magnetic resonance is known as the most sensitive method to probe electron paramagnetic resonance (EPR) and nuclear magnetic resonance (NMR). In these measurements, microcantilevers have been used as an ultrasensitive force sensor.[1] Magnetic resonance force microscopy (MRFM) is a typical example of such force-detected magnetic resonance, and single-spin sensitivity was achieved for impurities in silica, as demonstrated by Rugar *et al.*[2] MRFM is usually operated in the microwave region, but its frequency extension to the terahertz (THz) range is another promising application. Our group has developed high-frequency EPR techniques in the sub-THz and THz regions and demonstrated its usability for both crystalline and powder-like samples weighing 0.1–10 μg.[3–6]

As mentioned above, microcantilevers have been widely used for sensitive detection of magnetic resonance.[1–8] However, their application has been limited to solid-state samples because liquid-state samples have some inevitable difficulties in the setup. Namely, it is difficult to mount a small droplet precisely on a small cantilever platform. In addition, such a small droplet quickly evaporates in a few seconds, and hence it was practically impossible to keep the liquid phase on the cantilever while cooling the sample-holding cantilever. For these reasons, the applications of force-detected magnetic resonance to solution samples have not been reported. However, there is now a growing demand for highly sensitive measurements of small-volume solution samples in the research areas of biology and life science. For example, the biological functions of many proteins and enzymes are active only in solutions, where these molecules interact with the surrounding water.[9–11] In this sense, solution samples, rather than solid-state samples, must be measured in the case of proteins and enzymes to obtain more essential insights into their biofunctional activities.

Therefore, in this study, we developed a technique of ultrasensitive EPR spectroscopy applicable to solution samples in addition to solid-sate samples. For this purpose, a SiN_x nanomembrane and a liquid-sample cell were combined together to probe magnetic resonance signals without sample evaporation during setting. In this study, we demonstrated its usability for a microliter frozen solution of heme-containing samples, namely, hemin chloride and aquomet-myoglobin, at frequencies up to 350 GHz.

Figure 1 shows our experimental setup of a force-detected EPR system using a SiN_x nanomembrane specially developed for solution samples. In this study, a SiN_x nanomembrane (MEM-N03001/7.5M),[12] instead of microcantilevers, was used. The nanomembrane had lateral dimensions of 3 mm $\times$ 3 mm and a thickness of 100 nm and was fabricated on a 10 mm $\times$ 10 mm silicon substrate. The nominal spring constant and eigenfrequency were 100–150 N/m and 130–160 kHz, respectively. In this study, EPR signals were detected as a field gradient force acting between a sample and a gradient magnet.[13] A tiny drop of Stycast1266 (as a glue) was placed at the center of the SiN_x nanomembrane using a micro-injection pipette, and then, a strontium hexaferrite ($SrFe_{12}O_{19}$) sphere with a 40-μm diameter was mounted as a gradient magnet. After the gradient magnet was mounted, the eigenfrequency of the membrane decreased down to 1–10 kHz. Because $SrFe_{12}O_{19}$ is categorized as a soft magnetic material and its magnetization is almost (more than 90 percent) saturated at 0.3 T, the magnetic moment was fully oriented along the external magnetic field above 0.3 T.

The solution sample was injected into a small brass conical container. The top and bottom diameters were 7.5 and

a)Electronic mail: ohmichi@harbor.kobe-u.ac.jp

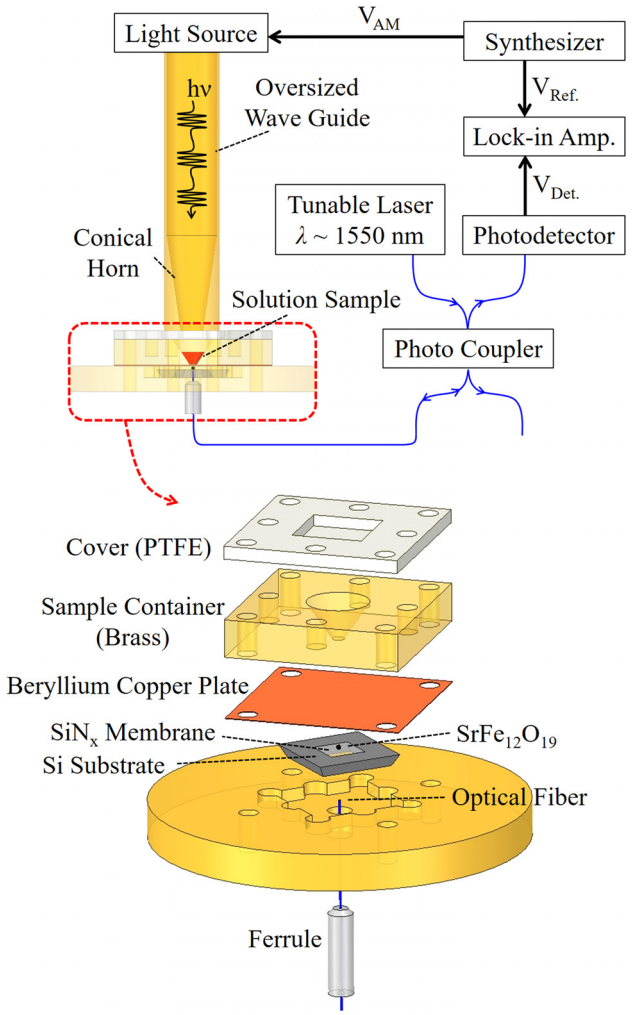

FIG. 1. Experimental setup of force-detected EPR spectroscopy for the solution sample using a SiN_x nanomembrane.

0.5 mm, respectively, and the height was 3.75 mm. The maximum sample volume was estimated to be about 55 μl. To prevent sample evaporation during preparation, the sample container was capped with a polytetrafluoroethylene (PTFE) plate with a thickness of 0.5 mm. It is noted that PTFE has a high transparency to electromagnetic waves in the sub-THz and THz ranges. The bottom side of the sample container was covered by a beryllium–copper plate with a 50-μm thickness. The magnetic interaction between the sample and the gradient magnet was possible through a thin beryllium–copper plate, but electromagnetic waves were shielded due to the skin effect. The role of shielding is twofold. One is to prevent ferromagnetic resonance of the strontium hexaferrite sphere on the nanomembrane. Without this shielding, additional absorptions would be superposed on the signals and the data analysis would be more complicated. The other role is to suppress spurious thermal nanomembrane vibrations. As explained later, the electromagnetic waves were amplitude-modulated so that direct irradiation of electromagnetic waves would induce spurious nanomembrane vibrations caused by the photothermal effect.

A field gradient force $\boldsymbol{F}$ acting between a gradient magnet and a sample is given by

$$\boldsymbol{F} = \nabla(\boldsymbol{B}_{\mathbf{tip}} \cdot \boldsymbol{M}), \tag{1}$$

where $\boldsymbol{B}_{\mathbf{tip}}$ is the magnetic field produced by a gradient magnet and $\boldsymbol{M}$ is the sample magnetization. In the EPR absorption process, electron spins are excited to the upper spin levels by absorbing electromagnetic waves and the magnetization of the spin system changes accordingly by ΔM_{EPR}. This is the basic principle of force-detected magnetic resonance. In our setup, a static magnetic field was applied normal to a nanomembrane, and sample magnetization was aligned to the same direction. Therefore, a field gradient component normal to the nanomembrane contributed to the field gradient force, according to Eq. (1), and the resultant field gradient force yielded a uniform deformation of the nanomembrane.

Figure 2 shows the contour plot of the field gradient component normal to the nanomembrane together with the shape of a brass container. It is found that the sign of the gradient changed at around 54°, which was slightly greater than the fabrication angle of 45° in this study. Therefore, it is noted that the field gradient components in the container were negative in most regions, whereas those outside of the container were positive. Thus, most of the sample volume in the container contributed to the unidirectional (attractive) force. Because the field gradient decays by the fourth-power law of the distance from a gradient magnet, samples located near the container bottom dominantly contribute to the force signals.

The field gradient at the bottom was typically 3.4 T/m, which was found to be much smaller than those in MRFM experiments.[1,2] As a result, the field distribution within 1 mm from the bottom was less than 0.24 mT, and the EPR spectra were affected little by the presence of the gradient field. This intentionally small gradient in our setup is important to acquire distortion-free high-resolution EPR spectra, which would become critical in detailed spectroscopic analyses.

Electromagnetic waves were introduced via an oversized stainless-steel pipe (diameter: 10 mm) and then were irradiated onto the sample through a brass horn (horn-end diameter: 4 mm). We used Gunn oscillators and backward traveling wave oscillators (BWOs) in the frequency ranges below and above 260 GHz, respectively. The nominal output power was 36 mW at 120 GHz, but decreased to 1–10 mW with increasing frequency.

To detect nanomembrane displacement, a home-built fiber-optic detection system was used.[4,5] A Fabry–Perot cavity was formed between the nanomembrane backside surface and the end of the optical fiber. The cavity length, typically kept at about 100 μm, was adjusted to the optimal position,

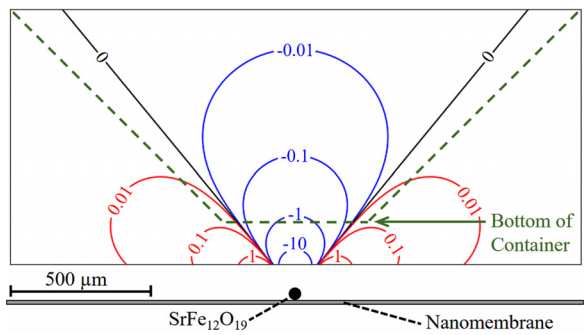

FIG. 2. Distribution of a gradient field produced by a 40-μm hexaferrite particle at around a brass sample container. The numbers on each contour represent the vertical component of field gradient in units of T/m.

where the photodetector output is proportional to the nanomembrane displacement. The laser wavelength was 1.5 μm. The typical detection sensitivity was on the order of 0.1 pm/$\sqrt{\text{Hz}}$ at 1 kHz.

Electromagnetic waves were amplitude-modulated using an internal modulator or a mechanical chopper for the Gunn oscillator and BWO, respectively. A modulation frequency of 13 Hz, which was far below the eigenfrequency of a magnet-on-membrane, was chosen to obtain flat baselines in a broad field range of interest. Reference signals from a synthesizer were fed to a lock-in amplifier and its synchronous photodetector signals were detected.

In this study, we measured frozen solution samples of hemin chloride and aquomet-myoglobin. Hemin is one of the model complexes of hemoproteins.[14,15] The sample purchased from Sigma Aldrich was dissolved in dimethyl sulfoxide (DMSO) and was prepared to a 50-mM concentration. Recombinant sperm whale myoglobin was expressed in *Escherichia coli* and purified as described previously.[16] A sample solution of 8.8-mM aquomet-myoglobin in 50-mM phosphate buffer (pH = 6.9) was prepared. In both cases, iron was trivalent (ferric) in the high-spin state (Fe^{3+}, $S = 5/2$).

Figure 3 shows the EPR spectra of frozen solution samples of hemin chloride (upper trace) and aquomet-myoglobin (lower trace) observed at 4.2 K. The field sweep rate was 0.5 and 0.2 T/min for hemin chloride and aquomet-myoglobin, respectively. The data acquisition was done for 0.3 s each for all data, and no signal averaging was performed. For hemin, the sample volume was 5 μl (2.5×10^{-7} mol). An asymmetric powder pattern was clearly observed at 120 and 210 GHz. The most intense signal observed in the low-field side was attributed to the $g_\perp$ signal, in which the magnetic field was applied perpendicular to the normal of the porphyrin plane, whereas the $g_\parallel$ signal, in which a magnetic field was applied parallel to the normal of the porphyrin plane, was obscured due to the low signal-to-noise ratio.

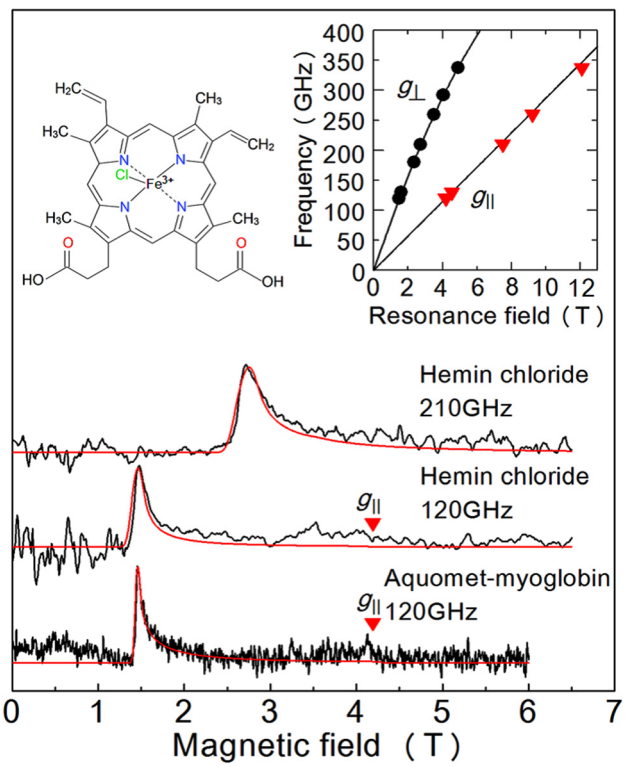

FIG. 3. EPR spectra (black) of frozen solution samples of hemin (upper trace) and aquomet-myoglobin (lower trace), together with simulated curves (red) with the reported parameters. In the EPR spectra of 120 GHz, the red triangles indicate the resonance field of $g_\parallel$ expected from numerical simulations. The molecular structure of hemin chloride is also shown. The inset shows the frequency-field diagram for hemin chloride. $g_\perp$ signals, shown by black circles, were experimentally determined, whilst $g_\parallel$ signals, shown by red triangles, were obtained by numerical simulations.

Hemin consists of a planar porphyrin ring with mostly C_{4v} symmetry, as shown in Fig. 3. Fe^{3+} ion is located at the center of the porphyrin plane and a chlorine atom is coordinated to Fe^{3+}.[17] For the high-spin ferric case, the spin Hamiltonian is given by

$$\boldsymbol{H} = \mu_B \boldsymbol{S} \cdot \boldsymbol{g} \cdot \boldsymbol{B} + D\boldsymbol{S}_z^2 + E(\boldsymbol{S}_x^2 - \boldsymbol{S}_y^2), \qquad (2)$$

where $\boldsymbol{g}$ is the g-tensor, μ_B is the Bohr magneton, and D and E are zero-field splitting (ZFS) parameters, respectively. A dominant source of the ZFS is spin–orbit interaction in transition metal complexes,[18,19] and the ZFS parameters have been experimentally determined by high-frequency EPR.[20–28] For the high-spin ferric case, the zero-field energy levels are described by three Kramers' doublets, separated by $2D$ and $4D$. The ZFS parameter for hemin chloride has been reported: $D \sim 6.90\,\text{cm}^{-1}$ and $E \sim 0.055\,\text{cm}^{-1}$.[28] The observed EPR spectra were reproduced well by the simulation curves (red line) using the reported parameters: $g_x = g_y = 1.93$, $g_z = 2.05$, $D = 6.90\,\text{cm}^{-1}$, and $E = 0.055\,\text{cm}^{-1}$).

For the aquomet-myoglobin solution sample, the sample volume was 10 μl, corresponding to a total spin number of 8.8×10^{-8} mol. We clearly observed a broad EPR spectra at 120 GHz. The apparent g factors, simply determined by the resonance field, were $g_\perp = 6$ and $g_\parallel = 2$,[29] which were similar to those of hemin chloride. This finding was reasonable because the EPR-active site of aquomet-myoglobin has a similar local structure with hemin, except that both sides of the porphyrin ring were coordinated by a water molecule and a histidine residue for aquomet-myoglobin.[30,31] It was found that the EPR line width of aquomet-myoglobin was sharper than that of hemin chloride. For aquomet-myoglobin, the porphyrin ring, which was surrounded by outer amino-acid chains, was isolated from each other, yielding negligible inter-molecule exchange interactions. For hemin chloride, on the other hand, the porphyrin rings were closely located, and the resultant non-negligible exchange interaction yielded a broadening of the EPR spectra.[32]

We plotted the frequency-resonance field diagram in the inset of Fig. 3 for hemin chloride. The resonance fields of the $g_\parallel$ signal were proportional to the frequency, whereas those of the $g_\perp$ signal exhibited an upward curvature in a different manner from conventional EPR signals. This behavior has been explained by the existence of D, the value of which could be precisely determined by numerical simulation curves as shown in the inset. In this sense, high-frequency EPR spectroscopy is very important to elucidate the intrinsic nature of the local electronic structure. Iron-containing proteins often possess large ZFS ($D \sim 1$–$10\,\text{cm}^{-1}$),[31,33–36] which is far above the energy scales of X-band microwaves. It was qualitatively expected that the apparent $g_\perp$ value would

approach the intrinsic g-value (g_x, g_y, and g_z) in the high-field limit ($\mu_B \boldsymbol{S} \cdot \boldsymbol{g} \cdot \boldsymbol{B} \gg D S_z^2$), where the Zeeman term surpasses the ZFS term.

Concentration sensitivity is an important factor to evaluate the applicability to solution samples.[37] In general, the concentration sensitivity of the high-frequency EPR spectrometer is worse than that of X- and Q-band EPR spectrometers because of the limited sample volume (<0.1 μl). To overcome this problem, a cavity-less W-band EPR system in which more sample volume (~10 μl) can be mounted has been reported to demonstrate the concentration sensitivity of 2 μM for TEMPO radical.[38] On the other hand, the concentration sensitivity achieved in this study was ~1.4 mM for aquomet-myoglobin, worse than the above-mentioned value and those needed for other spectroscopic methods such as solution NMR and UV-Vis absorption. However, the EPR spectra of aquomet-myoglobin was so broad (>2.5 T) that we would expect better concentration sensitivity of less than 1 μM for EPR species exhibiting narrower line width such as radicals.

Broad-band operation is another important factor from a viewpoint of ZFS parameters, because these parameters are strongly sample-dependent and have to be determined by multi-frequency EPR measurements. EPR detection of only 25-nl solution sample containing 1–10 mM high-spin ferric ions was reported at 275 GHz,[39] but the system equipped with a resonator can be operated at this fixed frequency. On the other hand, our technique can be operated in a broad frequency range up to 1 THz simply by replacing the millimeter-wave sources. In this sense, our force detection approach combined with a cavity-less setup will be a promising tool for spectroscopic studies of active centers of metalloproteins/enzymes in solutions.

For more practical applications, further sensitivity improvement would be necessary in the future. The use of high-power millimeter-wave sources such as gyrotron will be useful. Indeed, the output power of gyrotron (about 0.1–10 W) is 10^1–10^3 times stronger than that of Gunn oscillators. Another improvement will be the use of focusing elements of electromagnetic waves on the membrane. These technical improvements would give a better concentration sensitivity for metalloproteins/enzymes in practical levels (10–100 μM), and make it possible to study more detailed EPR analyses of scarce species in a small-volume solution.

In conclusion, we have developed a force-detected EPR technique for microliter solution samples using a SiN_x nanomembrane. We observed the EPR spectra of hemin chloride (50 mM, 5 μl) and aquomet-myoglobin (8.8 mM, 10 μl) in a broad frequency range up to 350 GHz with a high spectral resolution. This observation is an example of force-detected EPR spectroscopy of a frozen solution containing metalloproteins. The spin sensitivity, i.e., the detectable spin number divided by the line width, was on the order of 10^{11} spins/G. Thus, applications to other metalloprotein/enzyme solution samples are of particular interest in view of their biofunctional activities under hydrated conditions.

This study was partly supported by a Grant-in-Aid for Scientific Research (A) (No. JP17H01184) to Y.M., a Grant-in-Aid for Scientific Research (B) (No. JP26287081) to E.O., a Grant-in-Aid for Challenging Exploratory Research (No. JP26610104) to H.O., and a Grant-in-Aid for JSPS Research Fellow (No. JP18J11268) to T.O. from the Japan Society for the Promotion of Science (JSPS), the Asahi Glass Foundation to E.O., the Casio Foundation to E.O., and the Shimadzu Foundation to H.T.

[1]D. Rugar, C. S. Yannoni, and J. A. Sidles, Nature **360**, 563 (1992).
[2]D. Rugar, R. Budakian, H. J. Mamin, and B. W. Chui, Nature **430**, 329 (2004).
[3]E. Ohmichi, N. Mizuno, M. Kimata, H. Ohta, and T. Osada, Rev. Sci. Instrum. **80**, 013904 (2009).
[4]E. Ohmichi, Y. Tokuda, R. Tabuse, D. Tsubokura, T. Okamoto, and H. Ohta, Rev. Sci. Instrum. **87**, 073904 (2016).
[5]T. Okamoto, H. Takahashi, E. Ohmichi, and H. Ohta, Appl. Magn. Reson. **48**, 435 (2017).
[6]H. Takahashi, E. Ohmichi, and H. Ohta, Appl. Phys. Lett. **107**, 182405 (2015).
[7]S. Kuehn, S. A. Hickman, and J. A. Marohn, J. Chem. Phys. **128**, 052208 (2008).
[8]F. Hallak, J. van Slageren, and M. Dressel, Rev. Sci. Instrum. **81**, 095105 (2010).
[9]*High Resolution EPR, Applications to Metalloenzymes and Metals in Medicine*, edited by G. Hanson and L. Berliner (Springer, Berlin, 2009).
[10]K. Möbius and A. Savitsky, *High-Field EPR Spectroscopy on Proteins and their Model Systems: Characterization of Transient Paramagnetic States* (Royal Society of Chemistry, Cambridge, 2009).
[11]K. Möbius, A. Savitsky, A. Schnegg, M. Plato, and M. Fuchs, Phys. Chem. Chem. Phys. **7**, 19 (2005).
[12]See http://www.ntt-at.co.jp for information about SiN_x membrane chip.
[13]H. Takahashi, T. Okamoto, K. Ishimura, S. Hara, E. Ohmichi, and H. Ohta, Rev. Sci. Instrum. **89**, 083905 (2018).
[14]*Porphyrins and Metalloporphyrins*, edited by K. M. Smith (Elsevier, Amsterdam, 1975).
[15]W. S. Caughey, Annu. Rev. Biochem. **36**, 611 (1967).
[16]M. Kondoh, M. Mizuno, and Y. Mizutani, J. Phys. Chem. Lett. **7**, 1950 (2016).
[17]D. F. Koenig, Acta Cryst. **18**, 663 (1965).
[18]S. E. Stavretis, M. Atanasov, A. A. Podlesnyak, S. C. Hunter, F. Neese, and Z.-L. Xue, Inorg. Chem. **54**, 9790 (2015).
[19]F. Neese and E. I. Solomon, Inorg. Chem. **37**, 6568 (1998).
[20]J. Krzystek, A. Ozarowski, and J. Telser, Coord. Chem. Rev. **250**, 2308 (2006).
[21]A. Sienkiewicz, J. Krzystek, B. Vileno, G. Chatain, A. J. Kosar, A. S. Bohle, and L. J. Forró, J. Am. Chem. Soc. **128**, 4534 (2006).
[22]C. Duboc, T. Phoeurg, S. Zein, J. Pécaut, M.-N. Collomb, and F. Neese, Inorg. Chem. **46**, 4905 (2007).
[23]J. Krzystek, D. Smirnov, C. Schlegel, J. V. Slageren, J. Telser, and A. Ozarowski, J. Magn. Reson. **213**, 158 (2011).
[24]T. Okamoto, E. Ohmichi, Y. Saito, T. Sakurai, and H. Ohta, J. Phys. Chem. B **122**, 6880 (2018).
[25]J. Nehrkorn, J. Telser, K. Holldack, S. Stoll, and A. Schnegg, J. Phys. Chem. B **119**, 13816 (2015).
[26]J. Telser, J. V. Slageren, S. Vongtragool, M. Dressel, W. M. Reff, S. A. Zvyagin, A. Ozarowski, and J. Krzystek, Magn. Reson. Chem. **43**, S130 (2005).
[27]J. Telser, A. Ozarowski, and J. Krzystek, J. Biol. Inorg. Chem. **19**, 297 (2014).
[28]T. Okamoto, E. Ohmichi, S. Okubo, and H. Ohta, J. Phys. Soc. Jpn. **87**, 013702 (2018).
[29]T. Yonetani and H. Schleyer, J. Biol. Chem. **242**, 3926 (1967).
[30]R. E. Dickerson, *The Proteins* (Academic Press, New York, 1964).
[31]Y. Miyajima, H. Yashiro, T. Kashiwagi, M. Hagiwara, and H. Hori, J. Phys. Soc. Jpn. **73**, 280 (2004).
[32]J. Ernst, J. Subramanian, and J.-H. Fuhrhop, Z. Naturforsch., A **32**, 1129 (1977).
[33]J. Nehrkorn, B. M. Martins, K. Holldack, S. Stoll, H. Dobbek, R. Bittl, and A. Schnegg, Mol. Phys. **111**, 2696 (2013).
[34]P. J. M. van Kan, E. van der Horst, E. J. Reijerse, P. J. M. van Bentum, and W. R. Hagen, J. Chem. Soc., Faraday Trans. **94**, 2975 (1998).
[35]H. Hori, H. Yashiro, and M. Hagiwara, J. Inorg. Biochem. **116**, 53 (2012).
[36]G. C. Brackett, P. L. Richards, and W. S. Caughey, J. Chem. Phys. **54**, 4383 (1971).
[37]A. Blank, Y. Twig, and Y. Ishay, J. Magn. Reson. **280**, 20 (2017).
[38]L. Song, Z. Liu, P. Kaur, J. M. Esquiaqui, R. I. Hunter, S. Hill, G. M. Smith, and G. E. Fanucci, J. Magn. Reson. **265**, 188 (2016).
[39]G. Mathies, H. Blok, J. A. J. M. Disselhorst, P. Gast, H. van der Meer, D. M. Miedema, R. M. Almeida, J. J. G. Moura, W. R. Hagen, and E. J. J. Groenen, J. Magn. Reson. **210**, 126 (2011).